

Regional quantification of pulmonary biomechanics using dynamic MRI of grid-tagged hyperpolarized ^3He

G. W. Miller¹, J. Cai², T. A. Altes^{1,3}, E. E. de Lange¹, P. W. Read², K. Sheng², G. D. Cates^{1,4}, and J. P. Mugler, III¹

¹Department of Radiology, University of Virginia School of Medicine, Charlottesville, VA, United States, ²Department of Radiation Oncology, University of Virginia School of Medicine, Charlottesville, VA, United States, ³Department of Radiology, Children's Hospital of Philadelphia, Philadelphia, PA, United States, ⁴Department of Physics, University of Virginia, Charlottesville, VA, United States

Introduction: There is currently considerable interest in using lung MRI to study pulmonary biomechanics. In contrast with ^1H -based techniques [1,2], grid tagging of inhaled hyperpolarized ^3He provides a high signal, with a regular grid pattern in the lung that persists throughout the exhalation phase. Previous work demonstrated that maps of displacement, strain, and ventilation can be produced by comparing images of the grid pattern at inspiration and expiration [3]. The purpose of the present work is to develop a dynamic imaging strategy for tracking the evolution of 2D and 3D tagging grids at intermediate time points during the respiratory cycle, and to demonstrate the potential of this advanced technique for providing time-resolved, regional measurements of pulmonary biomechanics.

Methods: Dynamic imaging of both 2D and 3D tag motion was performed in two healthy volunteers (female, ages 29 and 32). To maximize sensitivity, 2D tagging grids were oriented in the sagittal plane, since the dominant lung motion occurs in the craniocaudal and anterior-posterior directions. MR imaging was performed using a 1.5T whole-body scanner (Siemens Sonata), and ^3He gas was polarized to approximately 40% using a commercial system (Model 9600, MITI). Following inhalation of a 1L mixture of $\sim 400\text{ml}$ hyperpolarized ^3He and $\sim 600\text{ml}$ N_2 , 2D or 3D tagging grids were created at breath hold, by applying sinc-modulated RF-pulse trains consecutively along any 2 or all 3 of the principal axes. Tag spacing was 18 mm for 2D tagging grids and 22 mm for 3D tagging grids.

Tag evolution was monitored during the subsequent exhalation, using a dynamic imaging sequence that combines radially symmetric k -space acquisition with angular under-sampling to accelerate the achievable frame rate (70ms per 2D slice acquisition). The idea behind this approach is that although image artifacts associated with the accelerated non-Cartesian trajectory may diminish overall image quality, they should not interfere with the ability to resolve the location of the high-signal regions defined by the tagging grid, which we refer to as "grid peaks". Multi-slice application of the 2D radial acquisition strategy was used to monitor 2D tags. Dynamic volumetric imaging of 3D tags was achieved by combining the angularly under-sampled acquisition in the radial plane with partial-Fourier phase encoding in the perpendicular direction to yield a reasonable 3D acquisition time ($<2\text{s}$).

Grid peaks in the 2D images were located and analyzed using an automated image reconstruction and processing procedure implemented in MATLAB. Manual intervention was occasionally required when grid elements overlapped or were severely distorted. Displacement maps were computed from the observed motion of the grid peaks, and maps of fractional ventilation were computed as $(V_1 - V_2)/V_1$, where V_1 and V_2 are the volumes of corresponding triangular grid elements at two different times. For 2D image sets, the principal components of strain (E_1 and E_2) were calculated from the observed deformation of the tagging grid.

Due to the complex nature of grid-peak movement in the 3D image sets, automated processing of these results is much more challenging. Routines for deriving the displacement maps are still under development.

Results/Discussion: Fig. 1a shows 2D tagged images from the right lung of subject #2, obtained at several different time points during exhalation. Distortion of the tagging grid at the fissure between the upper and lower lobes is evident in the later images (arrows) and in the map of the first principal component of strain (Fig. 1b). Fig. 1b indicates that the strain is uniformly small throughout each lobe. The anomalous values at the fissure likely reflect the relative motion of the lobes, rather than true strain within the lung tissue. The displacement map (Fig. 1c) reveals that the largest bulk motion occurs in the inferior portion of the lower lobe. The ventilation map (Fig. 1d) is more uniform than the displacement map throughout the interior of each lobe, which illustrates that although some regions of the lung move much farther than others during respiration, the local expansion is fairly uniform in normal pulmonary mechanics. The ventilation map also indicates that the lower lobe had slightly higher ventilation than the upper lobe. Fig. 2 shows the time evolution of mean ventilation, E_1 , and E_2 across a 2D slice from subject #1. Fig. 3 shows 3D tagging results from the same subject.

Conclusion: To our knowledge, this is the first use of dynamic MRI to track 2D and 3D motion of grid tags in the lung. Initial experience with the technique indicates that the use of an accelerated non-Cartesian trajectory to gain acquisition speed, at the cost of introducing image artifacts, provides a viable strategy for obtaining whole-lung coverage with reasonable temporal resolution. These preliminary results suggest that dynamic imaging of grid-tagged hyperpolarized magnetization is potentially a very powerful tool for observing and quantifying pulmonary biomechanics on a regional basis. Routines for automated analysis of the 3D data, which are currently being developed, may be particularly useful for analyzing alterations of pulmonary biomechanics in certain lung diseases.

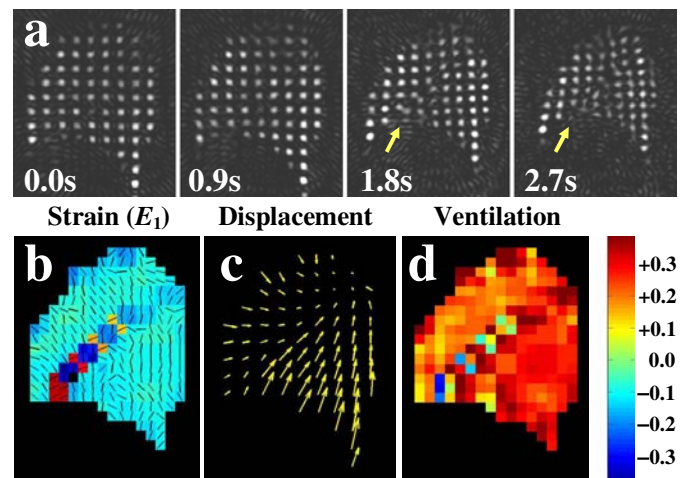


Figure 1: Sagittal slice from right lung of subject #2. (a) Time evolution of the 2D tagging grid during exhalation. Images were acquired at 64×64 pixel resolution with 33% angular sampling factor (35 radial views per image). Other imaging parameters: FOV 320mm, TR/TE 2.5/1.4ms, BW 780Hz/px, FA 3° . (b) Map of the first principal component of strain. (c) Displacement map. (d) Ventilation map. Color scale is the same for both (b) and (d).

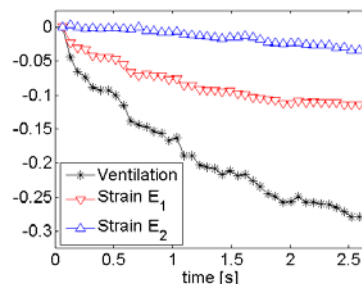
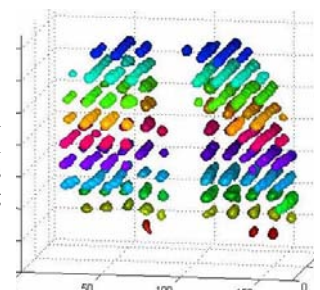


Figure 2: Temporal evolution of mean ventilation, E_1 and E_2 in subject #1.

Figure 3: Surface rendering of 3D tagging grid peaks, obtained from subject #1 early in the exhalation, that shows the size and distribution of the tagging grid throughout the lung. The underlying 3D images were acquired at $64 \times 64 \times 20$ pixel resolution, with 13 partial-Fourier phase-encoding partitions. The 49 radial views collected for each partition were divided into 7 interleaves, permitting sliding window reconstruction and a 3D pseudo-frame rate of 0.3s.



References: [1] Chen Q et al. MRM 2001; 45:24. [2] Kubo S et al. ISMRM 14 (2006); 6. [3] Cai J et al. ISMRM 14 (2006); 193.
Acknowledgments: Supported by NIH grant R01 HL079077 and Siemens Medical Solutions.